



iJRASET

International Journal For Research in
Applied Science and Engineering Technology



INTERNATIONAL JOURNAL FOR RESEARCH

IN APPLIED SCIENCE & ENGINEERING TECHNOLOGY

Volume: 13 Issue: VIII Month of publication: August 2025

DOI: <https://doi.org/10.22214/ijraset.2025.73523>

www.ijraset.com

Call:  08813907089

E-mail ID: ijraset@gmail.com

Performance Evaluation of Low-GWP HFO Refrigerants and Their Blends in a Subcooled Vapor Compression Cycle: A Python-CoolProp Simulation Approach

Akshat Tiwari¹, Dr. B.K. Chourasia²

¹Research Scholar, ²Professor & Head, Department of Mechanical Engineering, Jabalpur Engineering College, Jabalpur, Madhya Pradesh, India

Abstract: The environmental challenges posed by high-GWP refrigerants like R134a have necessitated the transition toward low-GWP alternatives, notably Hydrofluoroolefins (HFOs). This research presents a detailed simulation-based performance analysis of a Vapour Compression Refrigeration System (VCRS) incorporating a Liquid–Vapour Heat Exchanger (LVHE) to enable mechanical subcooling. Using Python and CoolProp, we compare the thermodynamic behavior of R134a, pure HFOs—R1234ze(E) and R1233zd(E)—and their binary blends across varying subcooling levels (0°C–30°C). An optimal subcooling value of 20°C is established, and a 70:30 blend of R1234ze(E) and R1233zd(E) is proposed as the most viable drop-in alternative to R134a. The results demonstrate substantial improvements in Refrigeration Effect (RE), Coefficient of Performance (COP), and system safety under optimized subcooling. Validation against published benchmarks ensures the reliability of the simulation approach. This study contributes a novel, environmentally conscious refrigerant blend optimized for subcooled VCRS applications, aligning with international climate mandates.

Keywords: HFO refrigerants, R1234ze(E), R1233zd(E), subcooling, LVHE, Python simulation, vapor compression system, sustainable refrigeration, R134a alternatives, low-GWP refrigerants.

I. INTRODUCTION

The escalating concern over global warming and ozone depletion has directed global attention toward replacing conventional refrigerants with sustainable alternatives. Hydrofluorocarbon (HFC) refrigerants like R134a, despite their favourable thermodynamic properties, exhibit high Global Warming Potentials (GWP \approx 1430), prompting their gradual phase-out as per international mandates such as the Kigali Amendment to the Montreal Protocol.

Among the promising alternatives are Hydrofluoroolefins (HFOs), such as R1234ze(E) and R1233zd(E), characterized by ultra-low GWPs (<10), zero Ozone Depletion Potential (ODP), and compatibility with existing system infrastructure. However, most current studies focus on either pure HFO refrigerants or traditional HFCs, HCs under standard operating conditions, with limited exploration into HFOs binary blends, specially under LVHE subcooled configurations.

To enhance energy performance while ensuring environmental compliance, this research integrates mechanical subcooling via a Liquid–Vapour Heat Exchanger (LVHE) within a single-stage Vapour Compression Refrigeration System (VCRS). Subcooling not only improves the Refrigeration Effect (RE) but also stabilizes the compressor operation and reduces entropy generation in downstream components (Çengel & Boles, 2014). Standard textbooks (Arora, 2013) and guidelines (ASHRAE, 2021) affirm the thermodynamic benefits of subcooling within a 5°C–20°C range.

This study builds upon the foundational methodology of Agarwal et al. (2021), which explored the energy and exergy behaviour of HFOs under varying subcooling degrees. Distinctively, our approach evaluates both pure and blended HFOs refrigerants using a Python–CoolProp simulation environment, proposing a novel 70:30 R1234ze(E)–R1233zd(E) blend as a thermodynamically and environmentally optimized alternative to R134a.

The paper systematically presents a simulation framework, performance comparison across refrigerant types and blend ratios, optimization of subcooling levels, and validation against benchmark studies. The findings aim to inform sustainable refrigerant selection and design optimization in future cooling systems.

II. LITERATURE REVIEW

The dual challenge of reducing environmental impact and improving energy efficiency in vapor compression refrigeration systems (VCRS) has directed recent research toward two promising strategies: the adoption of low-GWP refrigerants—especially hydrofluoroolefins (HFOs)—and the integration of subcooling techniques such as mechanical subcooling using Liquid–Vapour Heat Exchangers (LVHEs).

A. HFO Refrigerants and Drop-in Replacements

Several studies have examined HFOs such as R1234ze(E), R1234yf, and R1233zd(E) as drop-in or near drop-in alternatives to R134a. Belman-Flores et al. [1] reported that R1234ze(E) yielded a 13% higher Coefficient of Performance (COP) and a 5% reduction in Total Equivalent Warming Impact (TEWI) in domestic refrigerators. Yi et al. [13] found that R1234ze(E) outperformed R1234yf in centrifugal compressors with lower losses in system COP. Pundkar et al. [10] and Mota-Babiloni et al. [24] demonstrated that blends such as R513A and R450A could maintain compatibility with existing infrastructure while offering lower GWP and acceptable thermodynamic behavior. Experimental investigations by Agarwal et al. [4] and Mishra and Khan [21] validated that R1234ze(E) and R1234yf can match or exceed the efficiency of R134a in mechanically subcooled cycles, particularly when subcooling was introduced via LVHEs. Gupta et al. [20] emphasized the need for system-level optimization as pure HFOs often require higher input power despite their environmental advantages.

B. Subcooling Techniques for Performance Enhancement

Subcooling enhances the refrigerant's enthalpy of evaporation and reduces vapor content at compressor inlet, thereby improving system stability and efficiency. Solanki et al. [2] and Mogaji et al. [26] demonstrated that dedicated mechanical subcooling (DMS) increased COP by 9–33% while decreasing specific energy consumption. Sumeru et al. [18] reviewed multiple subcooling methods and ranked condensate-assisted subcooling (CAS) and mechanical subcooling via LVHEs among the most practical for integration with low-GWP refrigerants. In their numerical analysis, Tarish et al. [6] quantified the reduction in exergy destruction across compressor and condenser segments when R1234ze(E) and R1234yf were used with subcooling. Çengel & Boles (2014) and Arora (2013) theoretically affirm this behavior, where subcooling increases the refrigerant's specific enthalpy difference across evaporator sections without increasing pressure ratio.

C. Refrigerant Mixtures and Thermophysical Properties

Prasad et al. [3] and Farooq et al. [9] highlighted the potential of refrigerant blends, especially those combining R1234ze(E) with R1233zd(E), in achieving balanced thermal performance and environmental compliance. However, the success of such blends hinges on accurate thermophysical property estimation. Fedele et al. [22] and Bell et al. [15] emphasized the data scarcity in newer HFO blends, urging the use of open-source tools like CoolProp and REFPROP for simulation accuracy.

Recent modeling approaches by Allen et al. [23] and Olaoke et al. [27] demonstrated how Python-based frameworks and regression-based property models can effectively simulate real refrigerant behavior with reduced computational overhead—guiding the selection of simulation tools in this study.

D. Integration Challenges and Opportunities

Despite the promise of HFOs and subcooling, challenges persist. Mclinden et al. [25] and Gil & Kasperski [14] noted that no single refrigerant meets all ideal criteria—namely low GWP, high efficiency, low flammability, and material compatibility. Ghanbarpour et al. [8] further introduced the concept of a “critical emission factor,” implying that regional electricity emissions and power grid characteristics significantly influence refrigerant sustainability outcomes.

Moreover, Faraldo et al. [17] and Triki et al. [12] explored hybrid and solar-assisted VCR systems, highlighting the synergy between renewable energy inputs and low-GWP refrigerant selection, particularly in the context of subcooled designs.

III. SYSTEM CONFIGURATION AND METHODOLOGY

A. System Architecture and Working Principle

The simulated system is a single-stage Vapor Compression Refrigeration System (VCRS) integrated with a Liquid–Vapour Heat Exchanger (LVHE) for mechanical subcooling. The cycle consists of four primary components: evaporator, compressor, condenser, and expansion valve, augmented by the LVHE between the condenser and evaporator.

1) Schematic Diagram

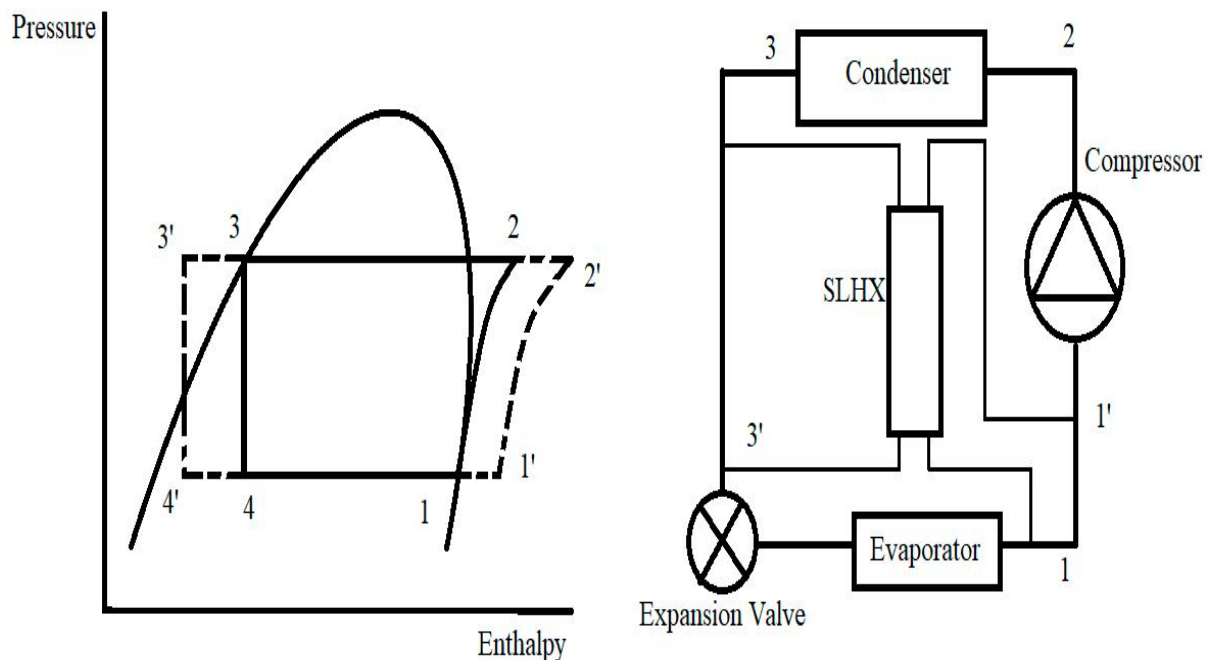


Fig. 1 The components Schematic diagram and pressure/enthalpy diagram of the VCC with a LVHE
Clean Technol. 2023

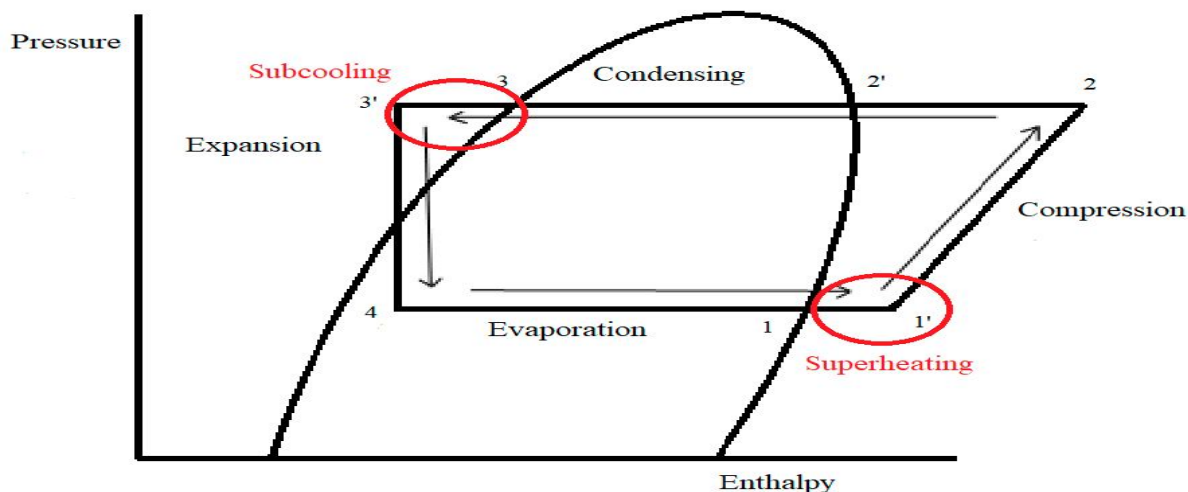


Fig. 2 The components Schematic diagram and pressure/enthalpy diagram of the VCC with a LVHE
Clean Technol. 2023

2) Working Process

- The high-pressure liquid refrigerant from the condenser is passed through the LVHE, where it is subcooled by exchanging heat with low-pressure vapor from the evaporator outlet.
- The subcooled liquid then enters the expansion valve, producing a lower vapor fraction at the evaporator inlet.
- The resulting lower vapor quality enhances the **Refrigeration Effect (RE)** due to increased latent heat absorption.
- In the LVHE, the low-pressure vapor exiting the evaporator transfers heat to the high-pressure liquid refrigerant from the condenser. This subcools the liquid before expansion, increasing the Refrigeration Effect (RE), and simultaneously superheats the vapor before compression, reducing the risk of liquid ingestion by the compressor (Çengel & Boles, 2014; Arora, 2013). The overall effect is a reduction in relative compressor work and an increase in system COP.

B. Simulation Assumptions

TABLE I
Assumptions Table

Assumption	Description
Steady-State	System operates in thermodynamic equilibrium
Isentropic Compressor	With fixed efficiency ($\eta = 0.8$)
Ideal Throttling	Isenthalpic expansion across expansion valve
No Heat Loss	Perfect insulation assumed across all components
Blend Approximation	Non-ideal effects neglected; properties calculated as mass-weighted averages
No Pressure Drop	Across condenser, LVHE, evaporator, and connecting pipes
Saturated Conditions	At condenser outlet and evaporator inlet

C. Operating Conditions

TABLE III
Operating Conditions

Parameter	Value
Net Cooling Capacity	3.5167 kW (1 TR)
Evaporator Temperature	-10°C
Condenser Temperature	50°C
Ambient Temperature	25°C
Subcooling Range	0°C to 30°C (in 5°C steps)
Blend Ratios {R1234ze(E):R1233zd(E)}	90:10 to 10:90 by mass
Subcooling Setpoint for Blend Analysis	20°C

D. Mathematical Model

Refrigerant Flow Convention in Present Work:

- 1) State 1: Vapor inlet to compressor (after superheating)
- 2) State 2s/2: Ideal/real outlet from compressor
- 3) State 3: Condenser outlet
- 4) State 3': Subcooled liquid (post-LVHE)
- 5) State 4: Expansion valve outlet
- 6) State 5: Evaporator outlet (before LVHE superheating)

a) Refrigeration Effect (RE):

$$\text{RE} = h_5 - h_4$$

Where h_5 is the specific enthalpy at the evaporator outlet, and h_4 is after throttling.

b) Compressor Work (W_{comp}):

$$W_{\text{comp}} = h_2 - h_1$$

Where h_2 is the specific enthalpy at the compressor outlet, and h_1 is at the compressor inlet.

c) COP (Coefficient of Performance):

$$\text{COP} = \text{RE} / W_{\text{comp}} = (h_5 - h_4) / (h_2 - h_1)$$

d) Subcooling Degree (ΔT_{sc}):

$$\Delta T_{\text{sc}} = T_3 - T_3'$$

The thermodynamic properties P, T, h, and s at all state points are calculated using **CoolProp** libraries within a Python environment.

E. Simulation Workflow

1) Baseline Simulation

Model R134a under subcooling degrees (0–30°C) for benchmark energy metrics.

2) Pure HFO Evaluation

Simulate R1234ze(E) and R1233zd(E) across the same subcooling range.

3) Blend Modeling

Approximate blend properties using:

$$X_{\text{blend}} = x \cdot X_{\text{ze}} + (1-x) \cdot X_{\text{zd}}$$

where “X” represents any property (h, s, T, P) and “x” the mass fraction of R1234ze(E).

4) Blend Ratio Analysis

Simulate and compare blend ratios (50:50, 60:40, 70:30, etc.) at 20°C subcooling to identify optimal configuration.

5) Thermodynamic Property Extraction

For each state point: T, P, h, s values computed and tabulated.

6) Energy Metrics Evaluation

Calculate RE, Compressor Work, and COP for each case.

7) Graphical Analysis

Generate plots:

- Subcooling vs RE
- Subcooling vs Compressor Work
- Subcooling vs COP
- Subcooling vs Superheating
- Blend Ratio vs RE
- Blend Ratio vs Compressor Work
- Blend Ratio vs COP

F. Validation Strategy

To ensure the credibility of the simulation framework:

- Compare COP values for R134a and R1234ze(E) with and without subcooling against results from Agarwal et al. (2021).
- Acceptable error margin $\leq \pm 1\%$ as CoolProp and REFPROP share common property formulations.

IV. RESULTS & DISCUSSION

This section presents a comprehensive quantitative and thermodynamic interpretation of simulation results across the refrigerants R134a, R1234ze(E), R1233zd(E), and their binary blends. The analysis is structured in three phases:

1) Baseline & Pure HFO Simulations (0–30°C subcooling)

2) Subcooling Optimization

3) Blend Performance Evaluation (at 20°C subcooling)

All simulations were performed using Python + CoolProp, and validation was ensured through comparative benchmarking with Agarwal et al. (2021). The difference in the values of COP is within the range of $\pm 1\%$.

A. Thermodynamic State Analysis

For each refrigerant, state points (1–5) were computed to obtain pressure (P), temperature (T), enthalpy (h), and entropy (s).

TABLE IIIII

R134a Thermodynamic States (0°C–30°C Subcooling)

Subcooling (°C)	State	T (°C)	P (bar)	h (kJ/kg)	s (kJ/kg·K)
0	1	-10.00	2.01	392.66	1.7334
	2s	57.06	13.18	431.96	1.7334
	2	65.60	13.18	441.79	1.7627
	3	50.00	13.18	271.62	1.2375
	3'	—	—	—	—

	4	-10.00	2.01	271.62	1.2734
	5	-10.00	2.01	392.66	1.7334
5	1	-0.83	2.01	400.47	1.7625
	2s	65.53	13.18	441.71	1.7625
	2	74.78	13.18	452.02	1.7925
	3	50.00	13.18	271.62	1.2375
	3'	45.00	13.18	263.90	1.2134
	4	-10.00	2.01	263.90	1.2440
	5	-10.00	2.01	392.66	1.7334
10	1	8.33	2.01	408.28	1.7907
	2s	74.20	13.18	451.39	1.7907
	2	84.04	13.18	462.17	1.8213
	3	50.00	13.18	271.62	1.2375
	3'	40.00	13.18	256.35	1.1895
	4	-10.00	2.01	256.35	1.2154
	5	-10.00	2.01	392.66	1.7334
15	1	17.50	2.01	416.15	1.8182
	2s	83.03	13.18	461.07	1.8182
	2	93.38	13.18	472.30	1.8493
	3	50.00	13.18	271.62	1.2375
	3'	35.00	13.18	248.97	1.1657
	4	-10.00	2.01	248.97	1.1873
	5	-10.00	2.01	392.66	1.7334
20	1	26.66	2.01	424.11	1.8452
	2s	91.98	13.18	470.78	1.8452
	2	102.78	13.18	482.45	1.8767
	3	50.00	13.18	271.62	1.2375
	3'	30.00	13.18	241.71	1.1419
	4	-10.00	2.01	241.71	1.1597
	5	-10.00	2.01	392.66	1.7334
25	1	35.83	2.01	432.16	1.8716
	2s	101.02	13.18	480.56	1.8716
	2	112.23	13.18	492.66	1.9035
	3	50.00	13.18	271.62	1.2375
	3'	25.00	13.18	234.57	1.1182
	4	-10.00	2.01	234.57	1.1326
	5	-10.00	2.01	392.66	1.7334
30	1	44.99	2.01	440.31	1.8976
	2s	110.15	13.18	490.41	1.8976
	2	121.72	13.18	502.94	1.9298
	3	50.00	13.18	271.62	1.2375
	3'	20.00	13.18	227.53	1.0944
	4	-10.00	2.01	227.53	1.1058
	5	-10.00	2.01	392.66	1.7334

TABLE IVV
R1234ze(E) Thermodynamic States (0°C–30°C Subcooling)

Subcooling (°C)	State	T (°C)	P (bar)	h (kJ/kg)	s (kJ/kg·K)
0	1	-10.00	1.47	377.25	1.6747
	2s	50.00	9.97	412.86	1.6747
	2	55.81	9.97	421.77	1.7021
	3	50.00	9.97	269.64	1.2315
	3'	—	—	—	—
	4	-10.00	1.47	269.64	1.2658
5	5	-10.00	1.47	377.25	1.6747
	1	-1.31	1.47	384.72	1.7026
	2s	55.97	9.97	421.95	1.7026
	2	64.50	9.97	431.25	1.7305
	3	50.00	9.97	269.64	1.2315
	3'	45.00	9.97	262.25	1.2085
10	4	-10.00	1.47	262.25	1.2377
	5	-10.00	1.47	377.25	1.6747
	1	7.39	1.47	392.27	1.7300
	2s	64.33	9.97	431.06	1.7300
	2	73.31	9.97	440.76	1.7583
	3	50.00	9.97	269.64	1.2315
15	3'	40.00	9.97	254.99	1.1855
	4	-10.00	1.47	254.99	1.2101
	5	-10.00	1.47	377.25	1.6747
	1	16.08	1.47	399.92	1.7568
	2s	72.82	9.97	440.24	1.7568
	2	82.21	9.97	450.32	1.7856
20	3	50.00	9.97	269.64	1.2315
	3'	35.00	9.97	247.85	1.1625
	4	-10.00	1.47	247.85	1.1830
	5	-10.00	1.47	377.25	1.6747
	1	24.77	1.47	407.67	1.7832
	2s	81.43	9.97	449.48	1.7832
25	2	91.19	9.97	459.93	1.8123
	3	50.00	9.97	269.64	1.2315
	3'	30.00	9.97	240.81	1.1394
	4	-10.00	1.47	240.81	1.1562
	5	-10.00	1.47	377.25	1.6747
	1	33.47	1.47	415.51	1.8092
	2s	90.12	9.97	458.79	1.8092
	2	100.23	9.97	469.61	1.8385
	3	50.00	9.97	269.64	1.2315
	3'	25.00	9.97	233.86	1.1163

	4	-10.00	1.47	233.86	1.1298
	5	-10.00	1.47	377.25	1.6747
30	1	42.16	1.47	423.44	1.8347
	2s	98.89	9.97	468.17	1.8347
	2	109.31	9.97	479.36	1.8643
	3	50.00	9.97	269.64	1.2315
	3'	20.00	9.97	227.00	1.0931
	4	-10.00	1.47	227.00	1.1037
	5	-10.00	1.47	377.25	1.6747

TABLE V
R1233zd(E) Thermodynamic States (0°C–30°C Subcooling)

Subcooling (°C)	State	T (°C)	P (bar)	h (kJ/kg)	s (kJ/kg·K)
0	1	-10.00	0.30	428.18	1.8735
	2s	50.00	2.93	468.31	1.8735
	2	59.49	2.93	478.34	1.9042
	3	50.00	2.93	292.49	1.3295
	3'	—	—	—	—
	4	-10.00	0.30	292.49	1.3579
	5	-10.00	0.30	428.18	1.8735
5	1	-2.63	0.30	433.74	1.8943
	2s	55.87	2.93	475.08	1.8943
	2	67.31	2.93	485.41	1.9252
	3	50.00	2.93	292.49	1.3295
	3'	45.00	2.93	286.21	1.3099
	4	-10.00	0.30	286.21	1.3340
	5	-10.00	0.30	428.18	1.8735
10	1	4.74	0.30	439.38	1.9149
	2s	63.46	2.93	481.93	1.9149
	2	75.16	2.93	492.57	1.9460
	3	50.00	2.93	292.49	1.3295
	3'	40.00	2.93	279.98	1.2901
	4	-10.00	0.30	279.98	1.3103
	5	-10.00	0.30	428.18	1.8735
15	1	12.11	0.30	445.11	1.9353
	2s	71.10	2.93	488.86	1.9353
	2	83.04	2.93	499.80	1.9665
	3	50.00	2.93	292.49	1.3295
	3'	35.00	2.93	273.79	1.2702
	4	-10.00	0.30	273.79	1.2868
	5	-10.00	0.30	428.18	1.8735
20	1	19.48	0.30	450.93	1.9554
	2s	78.76	2.93	495.87	1.9554

	2	90.95	2.93	507.10	1.9868
	3	50.00	2.93	292.49	1.3295
	3'	30.00	2.93	267.65	1.2501
	4	-10.00	0.30	267.65	1.2635
	5	-10.00	0.30	428.18	1.8735
25	1	26.85	0.30	456.83	1.9753
	2s	86.46	2.93	502.95	1.9753
	2	98.88	2.93	514.48	2.0068
	3	50.00	2.93	292.49	1.3295
	3'	25.00	2.93	261.55	1.2298
	4	-10.00	0.30	261.55	1.2403
	5	-10.00	0.30	428.18	1.8735
30	1	34.22	0.30	462.81	1.9950
	2s	94.19	2.93	510.11	1.9950
	2	106.83	2.93	521.94	2.0267
	3	50.00	2.93	292.49	1.3295
	3'	20.00	2.93	255.50	1.2093
	4	-10.00	0.30	255.50	1.2173
	5	-10.00	0.30	428.18	1.8735

TABLE VI

Blend {R1234ze (E) + R1233zd (E)} In 50:50 Ratio, With 20°C Subcooling

State	T (°C)	P (bar)	h (kJ/kg)	s (kJ/kg·K)
1	22.13	0.89	429.30	1.8693
2s	80.09	6.45	472.68	1.8693
2	91.07	6.45	483.51	1.8996
3	50.00	6.45	281.06	1.2805
3'	30.00	6.45	254.23	1.1947
4	-10.00	0.89	254.23	1.2098
5	-10.00	0.89	402.72	1.7741

TABLE VII

Blend {R1234ze (E) + R1233zd (E)} In 60:40 Ratio, With 20°C Subcooling

State	T (°C)	P (bar)	h (kJ/kg)	s (kJ/kg·K)
1	22.66	1.00	424.97	1.8521
2s	80.36	7.15	468.04	1.8521
2	91.09	7.15	478.80	1.8821
3	50.00	7.15	278.78	1.2707
3'	30.00	7.15	251.55	1.1837
4	-10.00	1.00	251.55	1.1991
5	-10.00	1.00	397.62	1.7542

TABLE VIII

Blend {R1234ze (E) + R1233zd (E)} In 70:30 Ratio, With 20°Csubcooling

State	T (°C)	P (bar)	h (kJ/kg)	s (kJ/kg·K)
1	23.18	1.12	420.65	1.8349
2s	80.63	7.86	463.40	1.8349
2	91.12	7.86	474.08	1.8646
3	50.00	7.86	276.50	1.2609
3'	30.00	7.86	248.86	1.1726
4	-10.00	1.12	248.86	1.1884
5	-10.00	1.12	392.53	1.7343

TABLE IX

Blend {R1234ze (E) + R1233zd (E)} In 80:20 Ratio, With 20°Csubcooling

State Point	T (°C)	P (bar)	h (kJ/kg)	s (kJ/kg·K)
1	23.71	1.24	416.32	1.8176
2s	80.90	8.56	458.76	1.8176
2	91.14	8.56	469.36	1.8472
3	50.00	8.56	274.21	1.2511
3'	30.00	8.56	246.18	1.1615
4	-10.00	1.24	246.18	1.1777
5	-10.00	1.24	387.44	1.7145

B. Energy Performance Metrics

The following metrics were evaluated across varying subcooling degrees:

$$\text{Refrigeration Effect (RE)} = h_5 - h_4$$

$$\text{Compressor Work (W)} = h_2 - h_1$$

$$\text{COP} = \text{RE}/\text{W} = (h_5 - h_4)/(h_2 - h_1)$$

Where h_1 , h_2 , h_4 , h_5 are the values of specific enthalpies at the respective state points.

TABLE X

R134a – Energy Performance (0°C To 30°C Subcooling)

Subcooling (°C)	Superheating (°C)	Refrigeration Effect (kJ/kg)	Compressor Work (kJ/kg)	COP
0	0.00	121.04	49.12	2.46
5	9.16	128.77	51.55	2.50
10	18.33	136.31	53.89	2.53
15	27.50	143.70	56.14	2.56
20	36.66	150.95	58.35	2.59
25	45.83	158.09	60.50	2.61
30	54.99	165.13	62.62	2.64

TABLE XI
R1234ze(E) – Energy Performance (0°C To 30°C Subcooling)

Subcooling (°C)	Superheating (°C)	Refrigeration Effect (kJ/kg)	Compressor Work (kJ/kg)	COP
0	0.0000	107.61	44.52	2.42
5	8.6933	115.00	46.54	2.47
10	17.3867	122.26	48.49	2.52
15	26.0801	129.40	50.40	2.57
20	34.7735	136.44	52.27	2.61
25	43.4669	143.39	54.10	2.65
30	52.1603	150.25	55.91	2.69

TABLE XII
R1233zd(E) – Energy Performance (0°C To 30°C Subcooling)

Subcooling (°C)	Superheating (°C)	Refrigeration Effect (kJ/kg)	Compressor Work (kJ/kg)	COP
0	0.0000	135.69	50.15	2.71
5	7.3690	141.97	51.68	2.75
10	14.7390	148.20	53.19	2.79
15	22.1090	154.39	54.68	2.82
20	29.4780	160.53	56.17	2.86
25	36.8480	166.63	57.65	2.89
30	44.2180	172.69	59.12	2.92

1) Refrigeration Effect

RE improved consistently with increased subcooling for all refrigerants, validating theoretical expectations ($RE = h_5 - h_4$).

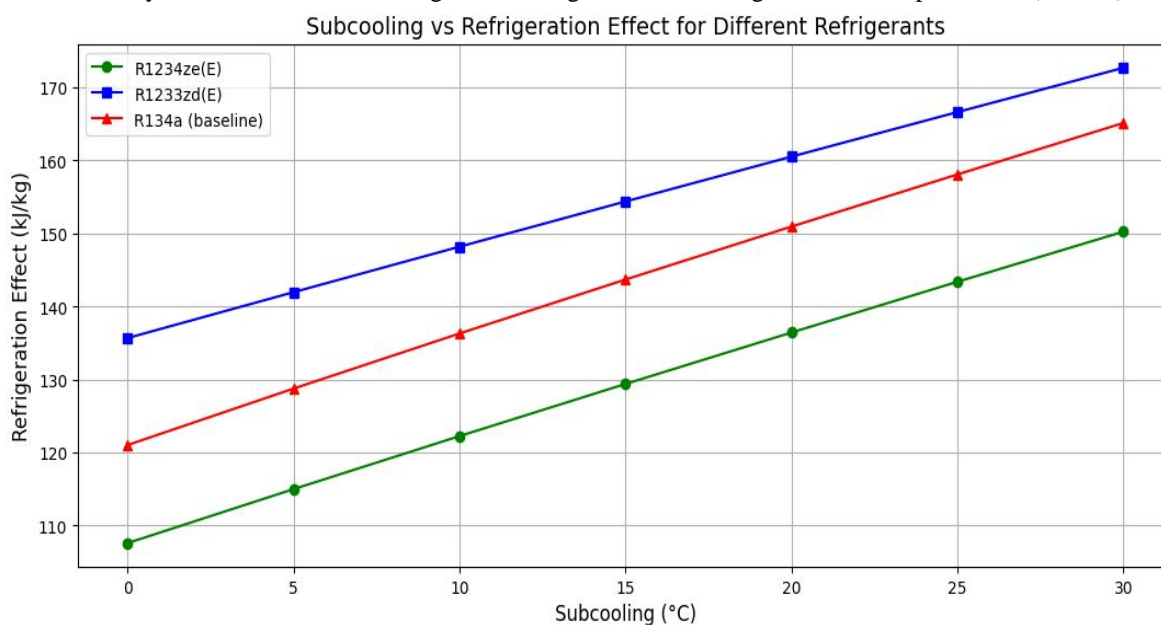


Fig. 3 Subcooling vs Refrigeration Effect for Different Refrigerants

2) Compressor Work Input

Compressor work ($W = h_2 - h_1$) showed an increasing trend with subcooling due to increased superheat after LVHE. HFOs showed moderate work increase compared to R134a.

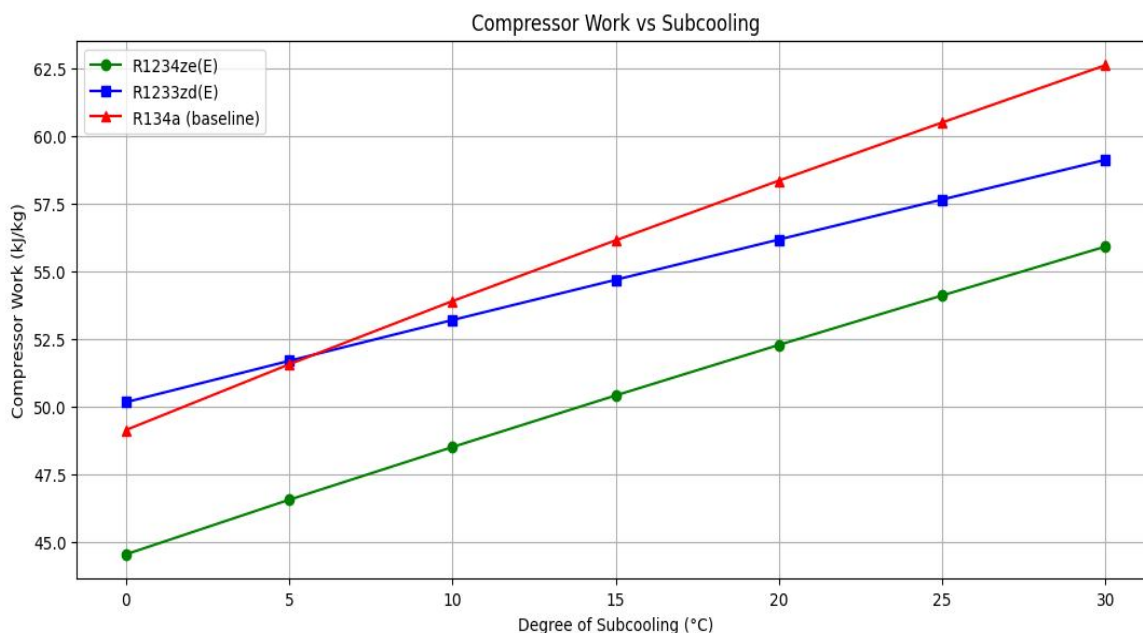


Fig. 4 Subcooling vs Compressor Work for Different Refrigerants

3) Coefficient of Performance (COP)

COP increased significantly with subcooling up to 20°C and then plateaued. This trend confirms prior studies (Agarwal et al., 2021) and ASHRAE design norms.

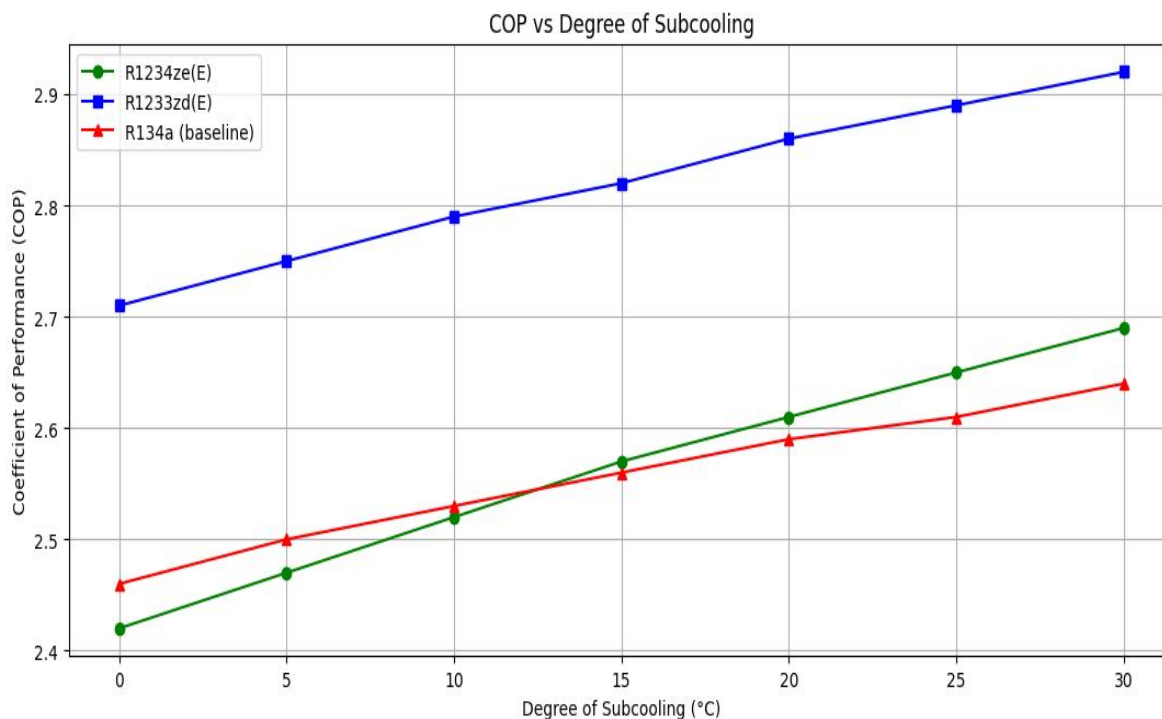


Fig. 5 Subcooling vs COP for Different Refrigerants

4) Superheating (SH)

Degree of superheat increases linearly with the increase in subcooling for all the refrigerants, since in the LVHE, heat rejected by the liquid line is equal to the heat absorbed by the vapour line.

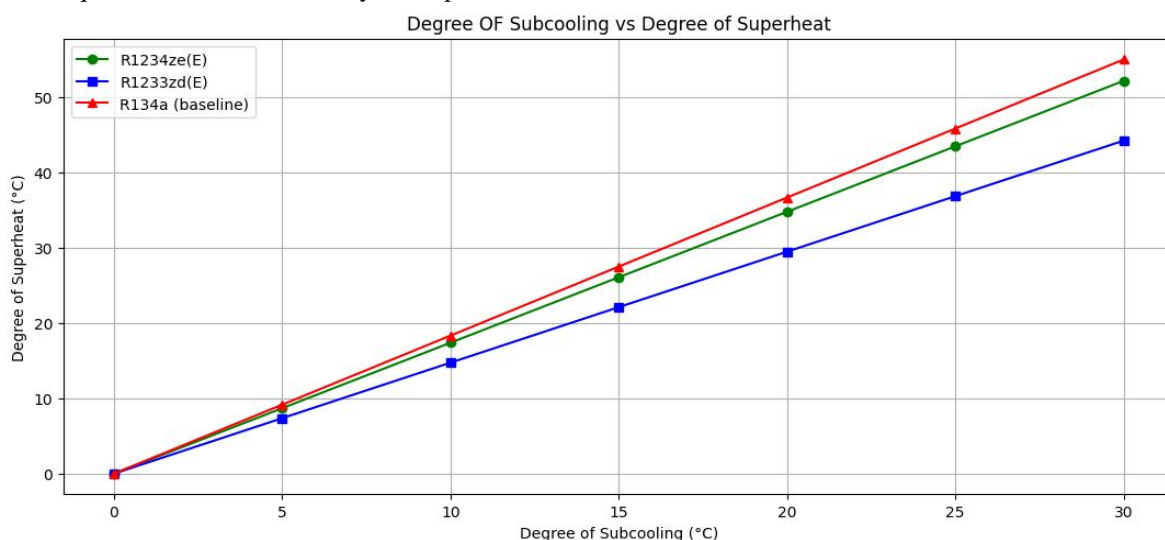


Fig. 6 Subcooling vs Superheating for Different Refrigerants

Interpretation: COP and RE improve with subcooling across all refrigerants. Compressor work also increases slightly due to vapor superheating in LVHE. The most optimal gains observed between 15–25°C subcooling range.

C. Subcooling Optimization

Simulation trends converge at **20°C subcooling**, balancing:

- Energy efficiency (maximizing RE, sustaining COP)
- System safety (avoiding liquid entry to compressor)
- Thermodynamic feasibility (valid LVHE operation)
- Compressor reliability (preventing excessive superheat)
- Academic alignment (ASHRAE, NIST, base paper validation)
- (ASHRAE Handbook (2021) and NIST REFPROP recommend 5–20°C subcooling for safe and effective system design.)

D. Blend Ratio Evaluation (at 20°C Subcooling)

Binary blends of {R1234ze(E):R1233zd(E)} were modeled from **90:10 to 10:90** using mass-weighted average property approximation.

TABLE XIII
Blend {R1234ze (E) + R1233zd (E) } At 20°C Subcooling

R1234ze (E) %	R1233zd (E) %	RE (Approx) (kJ/kg)	W (Comp.) (kJ/kg)	COP (Approx)
90	10	138.85	52.69	2.63
80	20	141.26	53.10	2.66
70	30	143.67	53.43	2.69
60	40	146.08	53.82	2.71
50	50	148.49	54.21	2.74
40	60	150.89	54.67	2.76
30	70	153.30	55.05	2.78
20	80	155.71	55.41	2.81
10	90	158.12	55.77	2.83

1) Refrigeration Effect

Refrigeration effect improves with increasing the proportion of R1233zd(E) in the blend [R1234ze(E)+R1233zd(E)]

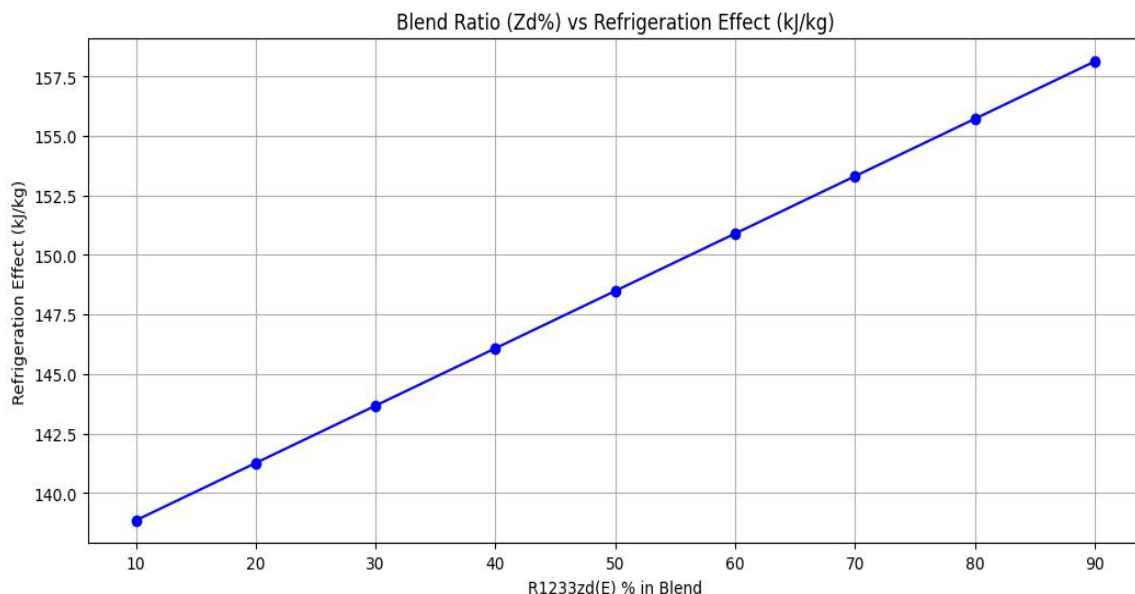


Fig. 7 Blend Ratio vs Refrigeration Effect for Different Ratio Proportions of Blend R1234ze(E)+R1233zd(E)

2) Compressor Work Input

Compressor work also increases with increasing the proportion of R1233zd(E) in the blend [R1234ze(E)+R1233zd(E)]

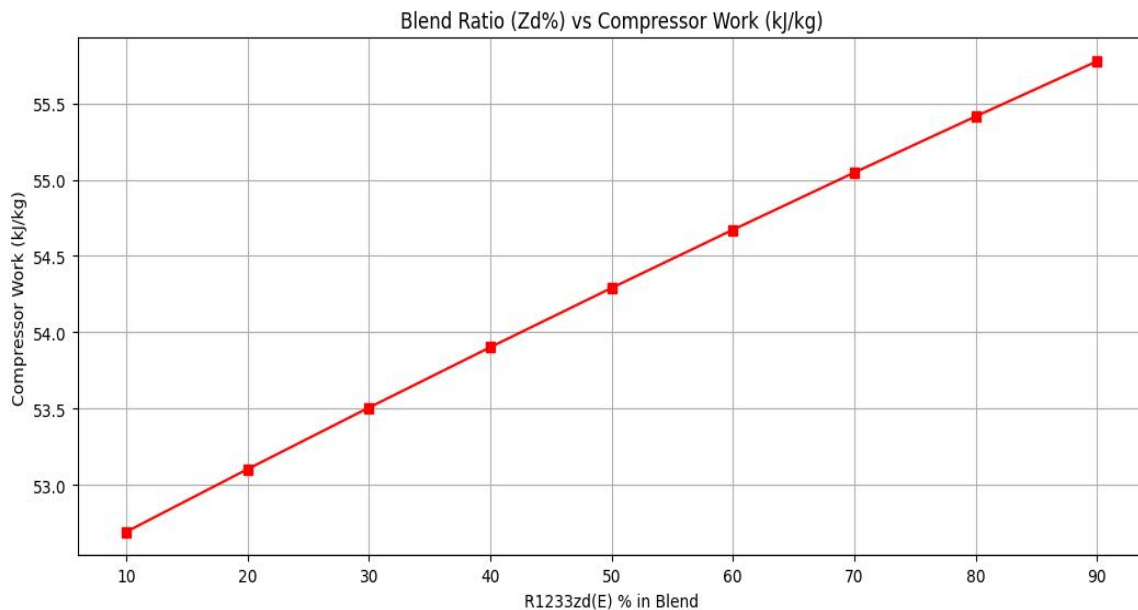


Fig. 8 Blend Ratio vs Compressor Work for Different Ratio Proportions of Blend R1234ze(E)+R1233zd(E)

3) Coefficient of Performance (COP)

Coefficient of performance increases with increasing the proportion of R1233zd(E) in the blend [R1234ze(E)+R1233zd(E)]. this tells, Although the compressor work increases slightly with increasing the proportion of R1233zd(E) in the blend [R1234ze(E)+R1233zd(E)], but the increasement of Refrigeration effect is dominating, thus results in increase of COP. This justifies the significance blending of R1233zd(E) in the pure HFO R1234ze(E).

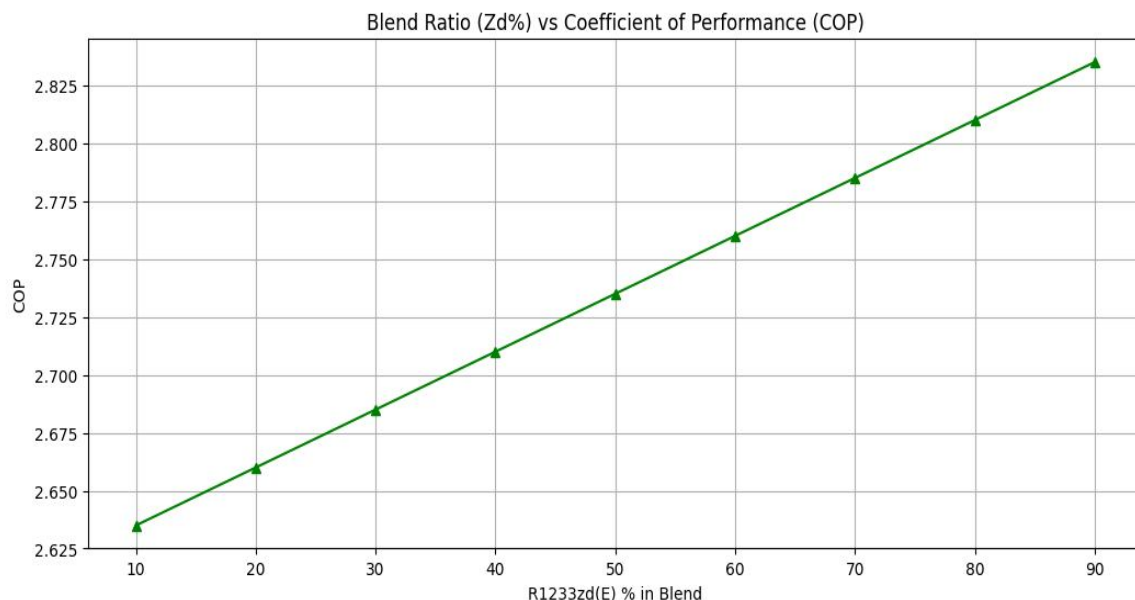


Fig. 9 Blend Ratio vs COP for Different Ratio Proportions of Blend R1234ze(E)+R1233zd(E)

E. Final Blend Selection Justification

Based on simulation and practical constraints:

Selected Blend: R1234ze(E) + R1233zd(E) in 70:30 (R1234ze(E):R1233zd(E)) mass ratio

Operating Subcooling: 20°C via LVHE

- Pressure Range:
 - Evaporator = 1.12 bar → Above atmospheric (Avoids sub-atmospheric evaporator pressures)
 - Condenser = 7.86 bar → Within design limits
 Pressures are within moderate range implies lesser loads on system components & safer operations.
- Safety: ASHRAE A2L category (mildly flammable, low-toxicity)
- Energy Metrics: Optimum Feasible Energy Performance Comparable or superior to R134a.

F. Comparative Performance Across All Refrigerants (Under Present Work Consideration)

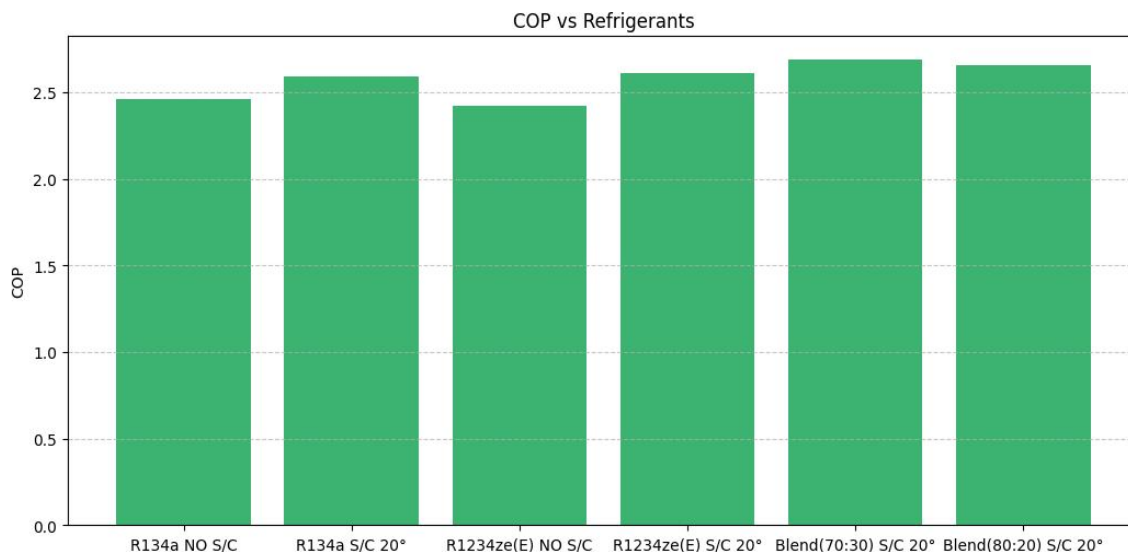


Fig. 10 COP Comparison: All Refrigerants

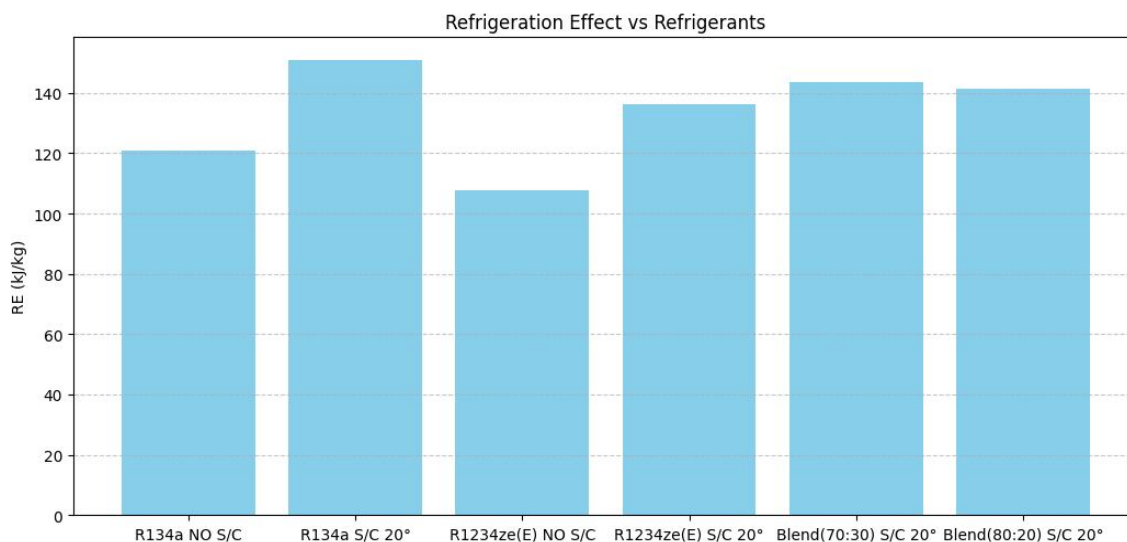


Fig. 11 Refrigeration Effect Comparison: All Refrigerants

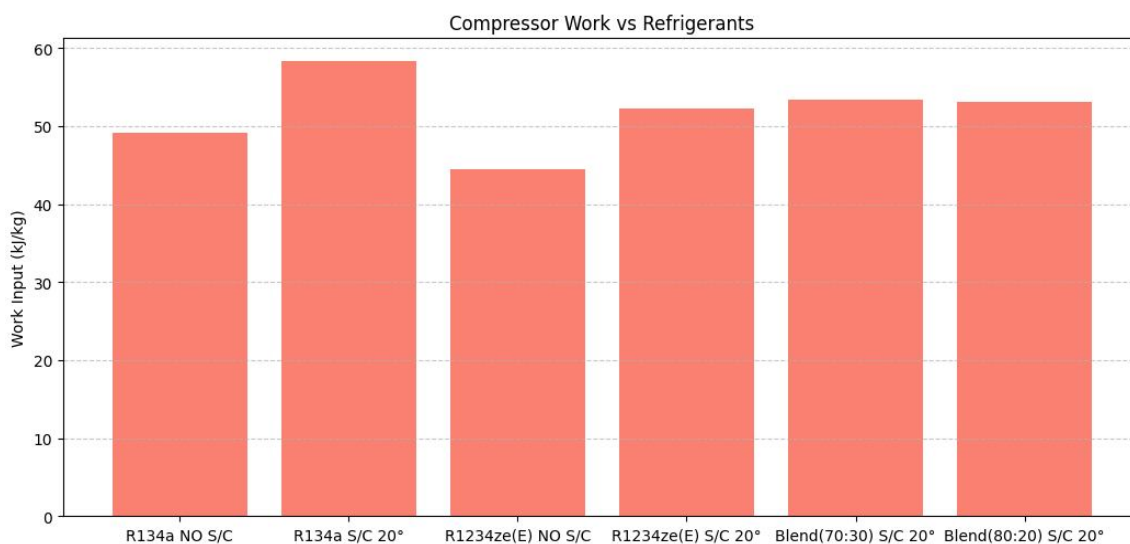


Fig. 12 Compressor Work Comparison: All Refrigerants

TABLE XIV

Energy Performance Summary Across All Different Considered Cases

Refrigerant	Subcooling (°C)	RE (Refrigeration Effect) (kJ/kg)	$W_{\text{compressor}}$ (kJ/kg)	COP	$P_{\text{Evaporator}}$ (bar)	$P_{\text{Condenser}}$ (bar)
R134a	0 (No S/C)	121.04	49.12	2.46	2.01	13.18
R134a	20	150.95	58.35	2.59	2.01	13.18
R1234ze(E)	0 (No S/C)	107.61	44.52	2.42	1.47	9.97
R1234ze(E)	20	136.44	52.27	2.61	1.47	9.97
Blend (70:30) [R1234ze(E):R1233zd(E)]	20	143.67	53.43	2.69	1.12	7.86

Key Result: Blend (70:30) at 20°C shows a 9.35% COP increase over R134a (no subcooling) and 3.86% over R134a (20°C subcooling) — making it the most technically and thermodynamically viable alternative.

V. CONCLUSIONS

This present work undertook a comprehensive simulation-based evaluation of low-GWP refrigerants and their blends in a Vapour Compression Refrigeration System (VCRS) enhanced with a Liquid–Vapor Heat Exchanger (LVHE). Based on the thermodynamic modeling, subcooling analysis, and blend simulations, the following conclusions are drawn:

The R1234ze(E):R1233zd(E) (70:30) blend at 20°C subcooling demonstrated the highest COP (2.69) and second-highest refrigeration effect (143.67 kJ/kg) among all tested configurations, while maintaining a favorable lower-moderate operating pressure range (1.12–7.86 bar). Compared to R134a at 0°C subcooling, the blend improved COP by 9.35% and refrigeration effect by 18.69%. When compared to R134a at 20°C subcooling, the blend still achieved a 3.86% higher COP and only a 4.82% lower refrigeration effect, while requiring 8.43% less compressor work. These performance metrics, combined with its ultra-low GWP and safety classification (A2L), make the blend a viable and sustainable replacement for R134a in modern VCR systems.

Trends matched previous empirical studies, notably that by Agarwal et al. (2021) verifying simulation correctness and academic robustness.

Practical implementation of this blend could be immediate for commercial refrigeration and chillers, requiring only minor design adaptations.

VI. NOMENCLATURE

Symbol / Abbreviation	Full Form (with Unit, if applicable)
COP	Coefficient of Performance (—)
RE	Refrigeration Effect (kJ/kg)
h	Specific Enthalpy (kJ/kg)
s	Specific Entropy (kJ/kg·K)
T	Temperature (°C or K)
P	Pressure (bar or Pa)
W_{comp}	Compressor Work Input (kJ/kg)
ΔT_{sc}	Subcooling Degree (°C)
VCRS	Vapour Compression Refrigeration System
LVHE	Liquid–Vapour Heat Exchanger
HFO	Hydrofluoroolefin
HFC	Hydrofluorocarbon
HC	Hydrocarbon
GWP	Global Warming Potential
ODP	Ozone Depletion Potential
TEWI	Total Equivalent Warming Impact
LCCP	Life Cycle Climate Performance
ASHRAE	American Society of Heating, Refrigerating and Air-Conditioning Engineers

VII. ACKNOWLEDGMENT

The author sincerely acknowledges the invaluable guidance and mentorship of **Dr. B.K. Chourasia**, Professor and Head, Department of Mechanical Engineering, *Jabalpur Engineering College, Jabalpur*. His deep technical insight, constant encouragement, and constructive feedback played a pivotal role in shaping this research work.

Gratitude is also extended to *Jabalpur Engineering College* for providing the academic environment and resources that enabled the successful completion of this study.

Special appreciation goes to the authors of the referenced literature whose meticulous work in the field of low-GWP refrigerants and subcooling techniques formed the scientific foundation of this research.

Lastly, heartfelt thanks to the author's parents for their enduring support, motivation, and belief throughout the academic journey.

REFERENCES

- [1] J. Belman-Flores, et al., "Drop-In Replacement of R134a in a Household Refrigerator with Low-GWP Refrigerants R513A, R516A, and R1234ze(E)," 2023.
- [2] K. Solanki, et al., "Performance Enhancement and Environmental Analysis of Vapor Compression Refrigeration System with Dedicated Mechanical Subcooling," 2023.
- [3] R. Prasad, et al., "Experimental and Simulation Study of the Latest HFC/HFO and Blend of Refrigerants in Vapour Compression Refrigeration System as an Alternative of R134a," 2023.
- [4] A. Agarwal, et al., "Energy and Exergy Investigations of R1234yf and R1234ze as R134a Replacements in Mechanically Subcooled Vapour Compression Refrigeration Cycle," 2020.
- [5] Y. Touaibi and H. Koten, "Energy Analysis of VCR System Using R1234yf and R1234ze as R134a Replacements," Journal of Advanced Research in Fluid Mechanics and Thermal Sciences, n.d.
- [6] A. Tarish, et al., "Exergy and Performance Analyses of Impact Subcooling for Vapor Compression Refrigeration System Utilizing Eco-Friendly Refrigerants," 2020.
- [7] M. Mclinden and M. Huber, "(R)Evolution of Refrigerants," 2020.
- [8] M. Ghanbarpour, et al., "Theoretical Global Warming Impact Evaluation of Medium and High Temperature Heat Pumps Using Low-GWP Refrigerants," 2021.
- [9] U. Farooq, et al., "Thermodynamic Performance Analysis of Hydrofluoroolefins (HFO) Refrigerants in Commercial Air-Conditioning Systems for Sustainable Environment," 2020.
- [10] A. Pundkar, et al., "Performance Evaluation of LGWP-Series Refrigerants as a Substitute for HFC-134a Air Conditioning System: A Sustainable Approach," 2025.
- [11] K. Alsouda, et al., "Vapor Compression Cycle: A State-of-the-Art Review on Cycle Improvements, Water and Other Natural Refrigerants," 2023.
- [12] M. Triki, et al., "Exergy Analysis of a Solar Vapor Compression Refrigeration System Using R1234ze(E) as an Environmentally Friendly Replacement of R134a," 2024.
- [13] J. Yi, et al., "Performance Evaluation of Centrifugal Refrigeration Compressor Using R1234yf and R1234ze(E) as Drop-In Replacements for R134a," 2022.
- [14] A. Gil and J. Kasperski, "Efficiency Evaluation of the Ejector Cooling Cycle Using a New Generation of HFO/HCFO Refrigerant as a R134a Replacement," 2018.
- [15] I. Bell, et al., "Survey of Data and Models for Refrigerant Mixtures Containing Halogenated Olefins," 2021.
- [16] T. Odunfa and O. Oseni, "Numerical Simulation and Performance Assessment of a Nanoparticle Enhanced Vapour Compression Refrigeration System," 2021.
- [17] S. Faraldo, et al., "Optimization of a Highly-Efficient Hydro-CO₂ Piston for Commercial Refrigeration," n.d.
- [18] M. Sumeru, et al., "A Review on Sub-Cooling in Vapor Compression Refrigeration Cycle for Energy Saving," 2019.
- [19] C. Aprea, et al., "HFO1234ze as Drop-in Replacement for R134a in Domestic Refrigerators: An Environmental Impact Analysis," 2016.
- [20] D. Gupta, et al., "Thermodynamic Analysis and Effects of Replacing HFC by Fourth-Generation Refrigerants in VCR Systems," 2018.
- [21] R. Mishra and M. Khan, "Theoretical Exergy Analysis of Actual Vapour Compression System with HFO-1234yf and HFO-1234ze as an Alternative Replacement of HFC-134a," 2016.
- [22] L. Fedele, et al., "Thermophysical Properties of Low GWP Refrigerants: An Update," 2023.
- [23] A. Allen, et al., "A Python-Based Code for Modeling the Thermodynamics of the Vapor Compression Cycle Applied to Residential Heat Pumps," 2023.
- [24] A. Mota-Babiloni, et al., "A Review of Refrigerant R1234ze(E) Recent Investigations," 2015.
- [25] M. Mclinden, et al., "New Refrigerants and System Configurations for Vapor-Compression Refrigeration," 2020.
- [26] A. Mogaji, et al., "COP Enhancement of Vapour Compression Refrigeration System Using Dedicated Mechanical Subcooling Cycle," 2020.
- [27] A. Olaoke, et al., "Computationally Efficient Property Calculation for Mixed Refrigerants Using Weighted Piecewise Polynomial Regression," 2024.
- [28] C. P. Arora, Refrigeration and Air Conditioning, 3rd ed., New Delhi: McGraw Hill Education, 2013.
- [29] Y. A. Çengel and M. A. Boles, Thermodynamics: An Engineering Approach, 9th ed., McGraw Hill Education, 2014.



10.22214/IJRASET



45.98



IMPACT FACTOR:
7.129



IMPACT FACTOR:
7.429



INTERNATIONAL JOURNAL FOR RESEARCH

IN APPLIED SCIENCE & ENGINEERING TECHNOLOGY

Call : 08813907089  (24*7 Support on Whatsapp)